Evaluation of the Role of His^{447} in the Reaction Catalyzed by Cholesterol Oxidase†

Ignatius J. Kass and Nicole S. Sampson*

Department of Chemistry, State University of New York, Stony Brook, New York 11794-3400

Received September 1, 1998; Revised Manuscript Received October 14, 1998

ABSTRACT: Cholesterol oxidase catalyzes the oxidation and isomerization of cholesterol to cholest-4-en-3-one via cholest-5-en-3-one. It has been proposed that His^{447} acts as the general base catalyst for oxidation, and that the resulting imidazolium ion formed acts as an electrophile for isomerization. In this work, we undertook an assessment of the proposed dual roles of His^{447} in the oxidation and isomerization reactions. To test its role, we constructed five mutants, H447Q, H447N, H447E, H447D, and H447K, that introduce hydrogen bond donors and acceptors and carboxylate bases at this position, and a sixth mutant, E361Q, to test the interplay between His^{447} and Glu^{361}. These mutants were characterized using steady-state kinetics and deuterium substrate and solvent isotope effects. For those mutants that catalyze either oxidation of cholesterol or isomerization of cholest-5-en-3-one, the K_m's vary no more than 3-fold relative to wild type. H447K is inactive in both oxidation (>100 000-fold reduced) and isomerization assays (>10 000-fold reduced). H447E and H447D do not catalyze oxidation (>100 000-fold reduced), but do catalyze isomerization, 10^4 times slower than wild type. The k_{cat} for H447Q is 120-fold lower than wild type for oxidation, and the same as wild type for isomerization. The k_{cat} for H447N is 4400-fold lower than wild type for oxidation, and is 30-fold lower than wild type for isomerization. E361Q does not catalyze isomerization (>10 000-fold reduced), and the k_{cat} for oxidation is 30-fold lower than wild type. The substrate deuterium kinetic isotope effects for the wild-type and mutant-catalyzed oxidation reactions suggest that mutation of His^{447} to an amide results in a change of the rate-determining step from hydride transfer to hydroxyl deprotonation. The deuterium solvent and substrate kinetic isotope effects for isomerization indicate that an amide at position 447 is an effective electrophile to catalyze formation of a dienolic intermediate. Moreover, consideration of kinetic and structural results together suggests that a hydrogen bonding network involving His^{447}, Glu^{361} and Asn^{485}, Wat^{541}, and substrate serves to position the substrate and coordinate general base and electrophilic catalysis. That is, in addition to its previously demonstrated role as base for deprotonation of carbon-4 during isomerization, Glu^{361} has a structural role and may act as a general base during oxidation. The His^{447}, Asn^{485}, Glu^{361}, and Wat^{541} residues are conserved in other GMC oxidoreductases. Observation of this catalytic tetrad in flavoproteins of unknown function may be diagnostic for an ability to oxidize unactivated alcohols.

Cholesterol oxidase (EC 1.1.3.6) is secreted by Gram-positive bacteria, e.g., *B. sterolicum* and *Streptomyces sp*. These bacteria can utilize cholesterol as their carbon source. More importantly for humans, it is the reagent employed to determine serum cholesterol levels, and has been in use for approximately 25 years. A second commercial use is on the horizon; the active enzyme is a potent larvicide. Upon ingestion by larvae of the Coeloptera family, e.g., boll weevils, their gut endothelia lyse (*1, 2*). Cholesterol oxidase has also been used as a probe of membrane structure and cholesterol content (*3*). Thus, understanding its mechanism is important for the development of new biotechnology products, as well as understanding the function of cell membranes at a molecular level.

Cholesterol oxidase (chox)[1] catalyzes the oxidation and isomerization of cholesterol to form cholest-4-en-3-one (Scheme 1). The 3β-hydroxyl is oxidized with concomitant reduction of FAD, and the reduced flavin is reoxidized by O_2 to yield 1 mol of H_2O_2 per mole of cholesterol. The formation of peroxide is the basis for enzymatic assays, both commercial and investigatory. Chox is a member of the GMC oxidoreductase family, that includes glucose oxidase, glucose dehydrogenase, choline dehydrogenase, and methanol oxidase (*4*, *5*). The primary regions of sequence similarity

† This work is supported by NIH Grant HL-53306, and in part by an American Heart Grant-in-Aid, a Camille and Henry Dreyfus New Faculty Award, and NSF Grant MCB-9405394 (N.S.S.). I.J.K. is a DOE/GAANN fellow. The NMR Spectroscopy facility at SUNY Stony Brook is supported by a grant from the NSF (CHE 9413510). The Spex fluorimeter was purchased with a grant from the NSF (CHE 9709164).

* To whom correspondence should be addressed. Telephone: (516) 632-7952. Fax: (516) 632-5731. E-mail: nicole.sampson@sunysb.edu.

[1] Abbreviations: chox, cholesterol oxidase; choB, *Brevibacterium sterolicum* cholesterol oxidase; choA, *Streptomyces* cholesterol oxidase; DHEA, dehydroepiandrosterone (3β-hydroxyandrost-5-en-17-one); LB, Luria broth; IPTG, isopropyl β-D-thiogalactoside; Tris, tris(hydroxymethyl)aminomethane; SDS−PAGE, sodium dodecyl sulfate−polyacrylamide gel electrophoresis; DEAE, diethylaminoethyl; TEA, triethanolamine; EDTA, ethylenediaminetetraacetate; HPLC, high-pressure liquid chromatography; TLC, thin-layer chromatography; HRP, horseradish peroxidase; 2 × YT, 2× yeast−tryptone broth; BSA, bovine serum albumin; GMC, glucose−methanol−choline; FAD, flavin adenine dinucleotide; EIMS, electron impact mass spectrometry; EI(HR), high-resolution electron impact mass spectrometry; OPA, opal stop codon; IR, infrared; NMR, nuclear magnetic resonance.

10.1021/bi982115+ CCC: $15.00
Published on Web 12/04/1998

Scheme 1

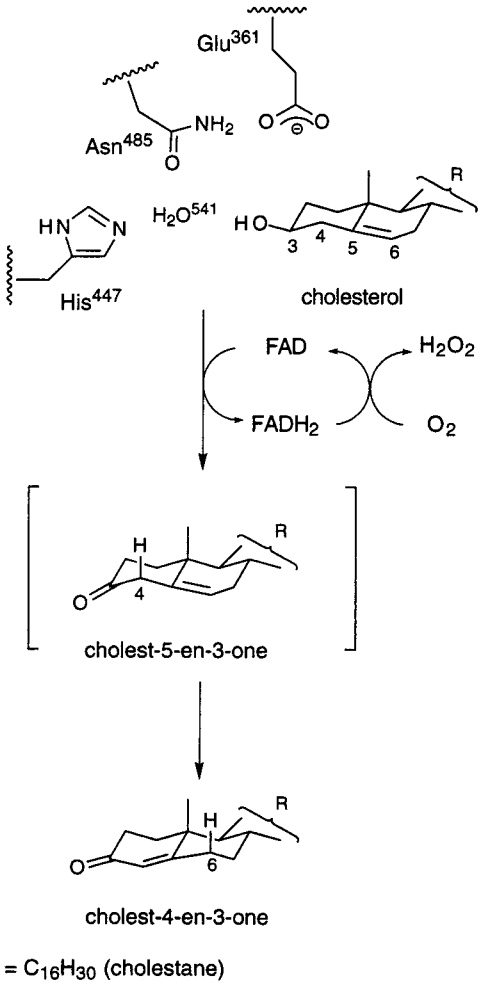

comprise the FAD-binding domain. Although there is little primary sequence similarity between cholesterol oxidase and the other family members in the substrate-binding site, there are tertiary structural similarities between glucose oxidase and cholesterol oxidase in the active sites (*6*). These similarities reflect the parallels between the oxidation reactions catalyzed by these enzymes. On the basis of the structural comparison of these two enzymes, it appears that His[447], Asn[485], and Glu[361] are highly conserved across the family, although they are not identical in every case (*7*).[2]

Previously, we investigated the chemistry of the isomerization reaction and the role of Glu[361]. The isomerization of cholest-5-en-3-one to cholest-4-en-3-one catalyzed by chox is stereospecific, and is catalyzed by one base via a dienolic intermediate. This was demonstrated with a deuterium transfer experiment. In the wild-type reaction, 30% of the deuterium at the 4β-position of cholest-5-en-3-one is transferred to the 6β-position of cholest-4-en-3-one; the remainder is lost to solvent (*11*, *12*). If 4α-[^{2}H]cholesterol is used, the deuteron is not transferred. The three-dimensional structure of chox suggested that Glu[361] could act as the base for isomerization because it is positioned over the β-face of the bound sterol (*5*). This role was confirmed by site-directed mutagenesis. When Glu[361] was substituted with Gln, the isomerization reaction was suppressed 10 000-fold; however, the oxidation reaction still occurred (*13*). Hence, the product of the E361Q reaction was cholest-5-en-3-one; moreover, it was produced catalytically. That is, the mutant enzyme released the intermediate of the wild-type reaction and was capable of multiple turnovers, although the mutant k_{cat} was 30-fold reduced from the wild-type k_{cat}. These experiments clearly demonstrated that Glu[361] is the catalytic base for isomerization.

The X-ray crystal structures of *Brevibacterium* chox (choB) solved by Blow and co-workers (*5*, *8*) and the *Streptomyces* (choA) structure solved by Yue et al. (Yue, K., Kass, I. J., Sampson, N. S., and Vrielink, A., personal communication) offer further insight into the mechanism. The structures of the native choB enzyme and of the DHEA-bound choB enzyme are very similar. In both structures, the active site is solvent-inaccessible. In the native structures of both choA and choB, the substrate-binding sites are filled with an identical water lattice. When a steroid is bound, 12 of these waters are displaced. Calculations suggest that displacement of these waters might provide the free energy for binding a hydrophobic moiety such as a steroid (*14*). These waters are sequestered from bulk solvent by two loops that appear to act as a lid to the binding cavity. Mutagenesis studies have shown that the larger loop (70−90) determines substrate specificity at the C17 end of the steroid. Deletion of this loop does not alter the stereospecificity of the isomerization reaction, or significantly change the percent of deuterium transferred between the 4β-position and the 6β-position. This suggests that the deuterium is washed out via a hydrogen bonding network through the protein, not through the binding site entrance. Conceptually, this is reasonable because the exchange reaction occurs when the binding site is occupied with substrate.

The structure of choB with DHEA bound reveals a hydrogen bonding network that connects the remaining water molecule in the active site with the conserved active-site residues His[447], Asn[485], and Glu[361] and the 3β-hydroxyl of the substrate (Figure 1). His[447] and Glu[361] are the only acidic or basic residues within 7 Å of the substrate hydroxyl. The position of His[447] suggests that it may act as a general base to remove the 3-hydroxyl proton via Wat[541] and catalyze electron transfer to FAD. The imidazolium that is formed could then act as a general acid to stabilize the formation of the dienolic intermediate during isomerization. Alternatively, the reaction intermediates may be stabilized by hydrogen bonds to Wat[541] and His[447] rather than complete proton transfer. Interestingly, wild-type chox catalyzes the isomerization of cholest-5-en-3-one to cholest-4-en-3-one with a k_{cat}/K_m that is less than 2-fold slower than the conversion of cholesterol to cholest-4-en-3-one; the k_{cat} is actually larger. The efficiency of cholest-5-en-3-one isomerization implies that the proton from the 3-hydroxyl is not required for isomerization.

The presence of the hydrogen bonding network shown in Figure 1 raises the possibility that Glu[361] may participate in an extended hydrogen bond network to the substrate hydroxyl through Wat[541] and Asn[485], and help catalyze oxidation. From the catalytic oxidation activity of the E361Q mutant, it is clear that Glu[361] is not essential for oxidation, but it may contribute as much as 2 kcal/mol to lower the activation

[2] This numbering refers to the X-ray crystal structure system for numbering amino acid residues (*8*). His[447] is encoded by codon 484 in the *Streptomyces* gene (*9*) and codon 492 in the *Brevibacterium* gene (*10*); Glu[361] is encoded by codons 398 and 406, respectively.

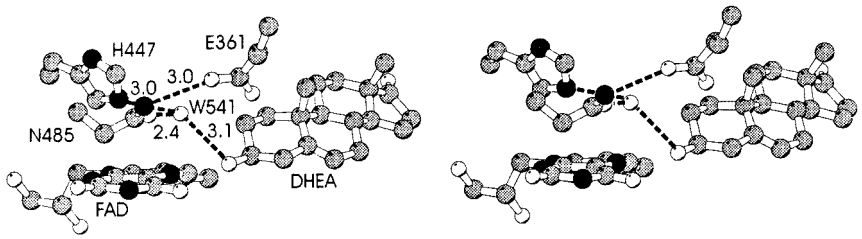

FIGURE 1: Divergent stereo figure of the X-ray crystal structure of *B. sterolicum* cholesterol oxidase with DHEA bound in the active site illustrating the hydrogen bonding network (*5*, *8*). Carbon is colored gray, oxygen is white, and nitrogen is black. Coordinates were obtained from the Brookhaven Protein Data Bank (1COY). The drawings were generated using MOLSCRIPT (*30*).

barrier of the reaction. Glucose oxidase catalyzes the oxidation of an unactivated alcohol, but does not catalyze isomerization of the oxidation product. Superposition of the glucose oxidase and cholesterol oxidase structures highlights the similarity of the catalytic residues in their active sites. His^{447} and Glu^{361} are strictly conserved, and the amide nitrogen of Asn^{485} is substituted with the Nδ of a histidine. The conservation of Glu^{361} in the active site of an enzyme that does not catalyze isomerization suggests that this basic residue has an additional purpose.

In this work, we undertook an assessment of the functional importance of His^{447} in catalysis, and the interplay between oxidation and isomerization. In addition, we assessed the extent to which Glu^{361} is involved in oxidation. To test the role of His^{447}, we constructed site-directed mutants to introduce hydrogen bond donors and acceptors, and carboxylate bases at this position. These mutants were characterized using steady-state kinetics, and primary solvent and substrate deuterium isotope effects. In addition, we have further characterized a previously described mutant, E361Q, in order to understand the proposed dual role of His^{447} as a general base for oxidation and a general acid for isomerization. The catalytic consequences that occur as a result of mutation are presented below. Our experiments suggest that imidazolium at position 447 is not required for isomerization; however, a hydrogen bond donor is necessary. The His^{447} base does contribute to catalysis during oxidation, although this residue is not essential. We propose that Glu^{361} also contributes to efficient catalysis of oxidation by organizing the water structure of the active site; and it may help to deprotonate the substrate oxygen. This additional role for Glu^{361} would explain its conservation in the GMC family, even in enzymes that do not catalyze 1,3 isomerizations.

EXPERIMENTAL PROCEDURES

Materials. Cholesteryl benzoate, cholest-4-en-3-one, cholest-5-en-3-one, $LiAl^2H_4$, NaB^2H_4, SeO_2, MnO_2, 4-aminoantipyrine, and Triton X-100 were from Aldrich Fine Chemical Co. (Milwaukee, WI). Cholesterol and horseradish peroxidase were purchased from Sigma Chemical Co. (St. Louis, MO). D_2O was from Cambridge Isotope Laboratories (D, 99.9%). The plasmid for heterologous expression of *Streptomyces* cholesterol oxidase, pCO202, has been described previously (*12*), and is a derivative of pCO117, a generous gift from Y. Murooka (*15*). Restriction endonucleases, T4 DNA ligase, calf intestinal alkaline phosphatase, and T4 kinase were purchased from New England Biolabs (Beverly, MA). Oligonucleotides were purchased from IDT, Inc. (Coralville, IA). All other chemicals and solvents, of reagent or HPLC grade, were supplied by Fisher Scientific (Pittsburgh, PA). Water for assays and chromatography was distilled, followed by passage through a Barnstead NANOpure filtration system to give a resistivity better than 18 MΩ.

General Methods. Diethyl ether was dried over and distilled from sodium/benzophenone ketyl under N_2 prior to use. Pyridine was dried over and freshly distilled from calcium hydride under N_2 prior to use. CD spectra were acquired on an Aviv Model 62A circular dichroism spectrophotometer. A Shimadzu UV2101 PC spectrophotometer was used for assays and acquisition of UV spectra. Fluorescence measurements were taken on a Spex Fluorolog 3-11 spectrofluorometer. The ^1H NMR and ^{13}C NMR spectra were recorded on Bruker AC-250, General Electric QE-300, Bruker AMX-600, Varian Gemini-300, or Varian Gemini-500 and referenced to $CDCl_3$ as the internal standard. ^1H NMR data are reported in the following manner: chemical shift in ppm (multiplicity, integrated intensity, coupling constant in hertz, and steroid carbon to which proton is attached). Only resolved steroid resonances are given. Restriction digests and ligations were performed according to procedures described in Sambrook et al. (*16*) The buffers used were as follows: buffer A, 50 mM sodium phosphate, pH 7.0; buffer B, buffer A + 0.025% Triton X-100 (w/v); C: buffer B + 0.020% BSA (w/v).

4β-[^{2}H]Cholest-5-en-3-one (17). A magnetically stirred solution of dry CH_2Cl_2 (400 μL) and dry pyridine (119 μL, 1.54 mmol) was cooled in an ice bath. A yellow−maroon color developed as CrO_3 (77 mg, 0.77 mmol) was slowly added as a solid. A solution of 4β-[^{2}H]cholesterol (*11*) (50 mg, 0.13 mmol) in dry CH_2Cl_2 (400 μL) was added dropwise and generated a green−black tar. The reaction was monitored by TLC, and all of the starting material was consumed after 20 min. The solvent was decanted, and additional CH_2Cl_2 (10 mL) was added to wash the green−black tar. The original liquid and the wash were filtered. The filtrate was extracted with 5% NaOH and 5% $NaHCO_3$. The solution was extracted with saturated $CuSO_4$ (5 mL) until there was no longer a change in the light blue color of the $CuSO_4$ solution. The solvent was removed on a rotary evaporator, and 16.2 mg (32% yield) of white solid was recovered after flash chromatography (7:93, EtOAc:mixed hexanes). ^1H NMR (300 MHz) δ 5.31 (bs, 1, C6), 3.25 (d, 0.12, $J_{4\alpha/4\beta} = 16.1$, C4$\beta$), 2.82 (d, 0.12, $J_{4\alpha/4\beta} = 16.6$, C4$\alpha$ with 4βH), 2.77 (s, 0.88, C4α with 4βD); EIMS 88 ± 5% D incorporation; EI-(HR) found 385.345144, calcd 385.345492.

Construction of H447N, H447D, H447E, and H447K ChoA Mutant Expression Plasmids, pCO227, pCO228, pCO229, and pCO235, Respectively. The *Bam*HI to *Nde*I fragment of pCO117 (*15*) containing the *Streptomyces* cholesterol oxidase choA gene was subcloned into pUC19

to generate pCO200. The extraneous *Streptomyces* DNA between the OPA and the *Hin*dIII site in pCO200 was removed by PCR using two primers. Primer 1 was a 50-base oligonucelotide that included the *Stu*I site within the choA gene and corresponded to the sequence of the coding strand (5′-AgCTgAAggCCTTCgCCgACgACTTCTgCTAc-**[A/g/T]A[A/T]**CCgCTCggCggCTgC-3′). The H447 codon was a mixture of bases that allowed mutation to Asn, Tyr, Lys, Asp, Glu, and Ochre. Primer 2 was a 27-base oligonucleotide that encoded the last 6 codons of the choA gene, incorporated a *Hin*dIII site with the OPA codon, and was complementary to the coding strand (5′-gCAgCAAgCTTACgACgCCgTgACgTC-3′). Using *Xho*I-restricted pCO117 as a template, 10 cycles of PCR were performed with Taq polymerase and an annealing temperature of 55 °C. The 216 bp PCR fragment was digested with *Stu*I and *Hin*dIII, purified, and subcloned into pCO200 (*12*) that had been similarly digested to yield the mutant expression plasmids containing the mutant *Streptomyces* choA genes behind a tac promoter. The individual mutants were identified by sequencing the 216 bp region synthesized by PCR using Sequenase v. 2.0 dideoxy termination sequencing following the manufacturer's protocol (US Biochemical, Cleveland, OH).

Construction of H447Q Mutant Expression Plasmid, pCO231. The H447Q choA was constructed as described above for the other H447 mutants except that primer 1 has the following sequence: 5′-AgCTgAAggCCTTCgCCgACgACTTCTgCTAc**CAg**CCgCTCggCgg-3′.

Construction of H447A Mutant Expression Plasmid, pCO234. The H447A choA was constructed as described above for the other H447 mutants except that primer 1 has the following sequence: 5-AgCTgAAggCCTTCgCCgACgACTTCTgCTAc**gCC**CCgCTCggCggCTgC-3′.

Purification of Wild-Type Cholesterol Oxidase. Cell paste of *E. coli* BL21(DE3)plysS(pCO202) was obtained from 1 L of 2 × YT−ampicillin (200 μg/mL) medium grown at 28 °C for 8 h after addition of IPTG (100 μg/mL) at $A_{600} = 1.0$ by centrifugation at 4000*g* for 30 min. The pellet was resuspended in 20 mL of buffer A and lysed by French press at 18 000 psi. All subsequent steps for wild-type cholesterol oxidase were conducted at 4 °C. Cell debris was removed by centrifugation at 135000*g* for 60 min. The supernatant was loaded onto a column of DEAE-cellulose (30 mm × 25 cm, DE-52, Whatman) preequilibrated with buffer A. Fractions were collected by elution with buffer A (100 mL). Typically, 15 mL fractions were collected; however, fractions that appeared yellow in color were limited to 7.5 mL. Fractions containing cholesterol oxidase (as determined by SDS−PAGE) were combined and concentrated by $(NH_4)_2SO_4$ precipitation (3.0 M). The pellet was redissolved in buffer A to give a final concentration between 10 and 20 mg/mL protein, and $(NH_4)_2SO_4$ was slowly added until the solution turned slightly turbid (typically, 2.5 M). The precipitate formed was pelleted by centrifugation, and the clarified supernatant was transferred to a fresh container where it was allowed to crystallize over 2 days at 4 °C. The microcrystalline protein was collected by centrifugation, dissolved in buffer A, and ultrafiltered (YM30 membrane, Amicon, Inc., Danvers, MA) into buffer A. The protein was further purified on a butyl-Sepharose column (30 mL butyl-Sepharose-4 Fast Flow, XK 16/40 column, Pharmacia Biotech, Upsala, Sweden) preequilibrated with 50 mM sodium phosphate, 1.0 M $(NH_4)_2SO_4$, pH 7.0. The protein was eluted by running a linear gradient from 50 mM sodium phosphate, 1.0 M $(NH_4)_2SO_4$, pH 7.0, to 100% buffer A (270 mL). Fractions were collected every 4.5 mL, and the elution profile was monitored at A_{280}. Fractions were assayed for content and purity by SDS−PAGE. Fractions containing pure cholesterol oxidase (>98%) were combined and ultrafiltered (YM30 membrane) into buffer A. Typically 30−40 mg of pure cholesterol oxidase was obtained per liter of culture. Protein concentrations were determined by UV absorbance using $\epsilon_{280} = 81\,924\ M^{-1}\ cm^{-1}$ [calculated from the molar extinction coefficients of tryptophan and tyrosine (*18*)].

Purification of Mutant Cholesterol Oxidases. Mutant cholesterol oxidases were prepared as described above for wild type. The yields of each mutant are as follows: E361Q, 25 mg/L; H447N, 9 mg/L; H447Q, 15 mg/L; H447E, 60 mg/L; H447D, 60 mg/L; H447K was expressed at such low levels (100 μg/L) that the purification was discontinued after the DE-52 column; H447A, no protein was detected in crude cell lysates or after initial purification steps. Protein concentrations were determined by UV absorbance using $\epsilon_{280} = 81\,924\ M^{-1}\ cm^{-1}$ [calculated from the molar extinction coefficients of tryptophan and tyrosine (*18*)].

UV and CD Spectra of Cholesterol Oxidase. Solutions of cholesterol oxidase were prepared in buffer A. A base line spectrum of buffer A was subtracted from the sample spectrum. The concentration of cholesterol oxidase was 13−23 μM for UV spectra and CD spectra in the near-UV. For CD spectra in the far-UV, the protein concentration was 13−58 μM. UV spectra were recorded from 600 to 200 nm. CD spectra were recorded in the near-UV from 300 to 255 nm, and in the far-UV from 250 to 183 nm.

Steady-State Enzyme Kinetics. Stock solutions of cholesterol and 3α-[^{2}H]cholesterol (approximately 4 and 2 mM) were prepared by dissolving cholesterol in propan-2-ol with magnetic stirring for 2 h. This solution was stored overnight at −20 °C and then filtered through a 0.45 μm nylon filter. The concentration of each solution was determined using cholesterol oxidase and standard assay condition 1 (vide infra). The results from six individual assays were averaged to determine the final concentration. Stock solutions of cholest-5-en-3-one and 4β-[^{2}H]cholest-5-en-3-one (2 mM) were prepared as above with the following exceptions. The solutions were prepared and stored in the dark in foil-wrapped containers. Because the cholest-5-en-3-one decomposes via autoxidation in solution (*13*, *19*), TLC (15:85, EtOAc:hexanes) or HPLC was employed to assay the solutions for purity prior to use each day.

p-Hydroxyphenylacetic acid (1.0 M), HRP (1000 units/mL), phenol (113 mM), and 4-aminoantipyrine (440 mM) stock solutions were prepared in buffer B. Dilute enzyme stock solutions were prepared in buffer C. The concentration of each enzyme used in assays with cholesterol and 3α-[^{2}H]-cholesterol was as follows: ChoA, 0.55 nM; H447Q, 53 nM; and E361Q, 10 nM. The concentration of each enzyme used in assays with cholest-5-en-3-one and 4β-[^{2}H]cholest-5en-3-one was the following: ChoA, 0.44 nM; H447Q, 0.53 nM; and H447N, 8.8 nM.

Initial velocities were measured in one of three ways. (1) The formation of conjugated enone was followed as a function of time at 240 nm [$\epsilon_{240} = 12\,100\ M^{-1}\ cm^{-1}$ (*20*)].

Cholesterol was added as a propan-2-ol solution (4 mM) to buffer C prewarmed to 37 °C. The final assay mixture was 3% propan-2-ol. (2) The formation of quinoneimine was followed at 510 nm using an HRP-coupled assay to quantitate the rate of formation of H_2O_2. The standard assay conditions were the same as the UV A_{240} assay with the addition of 1.13 mM phenol, 0.87 mM 4-aminoantipyrine, and 10 units of horseradish peroxidase. (3) The reaction was followed by excitation at 325 nm and monitoring the fluorescence emission at 415 nm (slits = 1.5 nm) using an HRP-coupled assay to quantitate the rate of formation of H_2O_2. The standard assay conditions were the same as the UV A_{240} assay with the addition of 1.0 mM *p*-hydroxyphenylacetic acid and 10 units of horseradish peroxidase. Independent sets of data were fit simultaneously to the hyperbolic form of the Michaelis−Menten equation using Grafit (Erithacus, London, U.K.). Primary isotope effects were determined in a similar fashion fitting all possibilities and selecting the best fit (^DV, $^DV/K$, or ^DV and $^DV/K$).

Determination of the pH Profile of Catalytic Activity. The catalytic activity of the enzymes was determined over a pH range of 2.6−10.8. Assays were prepared as described for general assays for the specific activity of cholesterol oxidase with the substitution of the appropriate pH buffers. Buffers used were 50 mM citrate−phosphate (pH 2.6−5.6), 50 mM phosphate (pH 6.5−8.0), and 50 mM glycine−NaOH (pH 8.5−10.8). Each buffer contained 0.025% (w/v) Triton X-100 and 0.02% (w/v) BSA. ChoA (1 nM) was assayed in buffer C containing 50 μM cholesterol utilizing the A_{240} assay. ChoA (2 nM), H447Q (4 nM), and H447N (18 nM) were assayed in buffer C containing 50 μM cholest-5-en-3-one utilizing the A_{240} assay. E361Q (35 nM) was assayed in buffer C containing 50 μM cholesterol and 176 nM H447N. Observed rates were corrected by subtracting the background rate of H447N activity.

HPLC Analysis. Samples were analyzed as previously described (*13*) with a Model 680 gradient controller, three M510 solvent pumps, and a Model 490 multiwavelength detector (Waters Corp., Milford, MA) or a Model PDA-1 photodiode array detector (Rainin Instrument, Woburn, MA). The following conditions were used: stationary phase, Microsorb-MV C-18 column (Rainin Instrument Corp., 5 μm, 10 Å, 4.6 × 250 mm); gradient elution at 1.25 mL/min; solvent A, CH_3CN; solvent B, propan-2-ol; solvent C, CH_3CN/H_2O (1:1, v/v); detection at 212 and 240 nm. Then 25 min isocratic elution with 80% A and 20% C followed by a 10 min linear gradient to 85% A and 15% B followed by 25 min isocratic elution at the same conditions was used to separate the steroids. Samples were injected directly from assay solutions. The identity of the peaks was established by co-injection with authentic standards. Product ratios were determined by integration of peak areas as detected at 212 and 240 nm.

Determination of Reaction Stereospecificity. Deuterium labeling experiments were conducted as previously described (*11*) except that 4β-[^{2}H]cholest-5-en-3-one (140 μM) was used. The steroid was incubated with 11 nM H447Q or 70 nM H447N in buffer A. The reaction was allowed to go to completion (0.5 h). The solution was extracted immediately with EtOAc (3 × 15 mL) and the solvent removed by rotary evaporation. The residue was redissolved in CH_3CN, and the product was isolated by HPLC and analyzed by EIMS, and ^{1}H NMR and IR spectroscopy. The position of deuterium incorporation was determined by the integration of ^{1}H resonances in the ^{1}H NMR spectrum.

Determination of Solvent Isotope Effects. Deuterated phosphate buffer was prepared by lyophilizing portions of buffer stocks and reconstituting with one-fifth the starting volume D_2O (2×) followed by a final reconstitution to the original volume with D_2O. The stocks were used to prepare buffer A at pD 7.0. The pD was adjusted by adding 0.4 to the pH meter reading (*21*). To exchange all enzyme-associated protons with deuterium, cholesterol oxidase was incubated at 37 °C overnight in D_2O buffer, monitored for retention of activity, lyophilized, and reconstituted with D_2O in the same manner as described above for buffer. The activity assays were performed as described above. In the fluorescence assay, it was necessary to recalculate the fluorescence change per micromole of dye dimer, because there was an isotope effect on the fluorescence quantum yield.

RESULTS

Preparation of Cholesterol Oxidase His^{447} Mutants. Point mutations were prepared by PCR cassette mutagenesis using existing restriction sites in pCO202 (*12*). The mutant cholesterol oxidases were heterologously expressed in *E. coli*. The levels of expression relative to wild-type cholesterol oxidase varied from mutant to mutant (0−60 mg/L of culture). There was no correlation between catalytic activity and expression level. The H447K mutant was expressed at such low levels (100 μg/L) that it was only minimally purified. The H447A mutant was not expressed at all. The other mutant cholesterol oxidases were purified in a manner similar to wild type. The purity of each mutant was confirmed by SDS−PAGE analysis and UV/vis and CD spectroscopy. The UV spectra of the bound FAD cofactors of the purified mutant cholesterol oxidases have λ_{max}'s identical to wild type at 391 and 468 nm. The CD spectra (far- and near-UV) show that all of the mutants are folded the same as wild type (data not shown). X-ray crystal structures of the H447N, H447Q, and E361Q mutants confirmed that they were folded identically to wild type (Yue, K., Kass, I. J., Sampson, N. S., and Vrielink, A., personal communication).

Analysis of Products Formed by Mutants. Comparisons of mutant activity with cholesterol as a substrate were made by measuring the rate of H_2O_2 formation using a horseradish peroxidase coupled assay, and by following the rate of cholest-4-en-3-one appearance at 240 nm. In the wild-type catalyzed reaction, the two assays measure identical rates. For the H447Q mutant, the two assays measured identical rates, implying that the mutant could convert cholesterol to cholest-4-en-3-one. The H447N mutant catalyzed oxidation very slowly with a specific activity 4400-fold below wild type. As previously described, the E361Q mutant does catalyze the oxidation reaction. However, the rate of cholest-4-en-3-one formation is at least 10 000-fold slower than the wild-type reaction (*13*). That is, catalytic activity was observed with the HRP assay, but not with the A_{240} assay. Within the detection limits of the assays, the H447K, H447E, and H447D mutants did not oxidize cholesterol and were at least 100 000-fold reduced in activity from wild type.

Table 1: Catalytic Capability of Wild-Type and Mutant Cholesterol Oxidases[a]

	cholesterol to cholest-5-en-3-one[b]	cholesterol to cholest-4-en-3-one[c]	cholest-5-en-3-one to cholest-4-en-3-one[c]
wild type	++++	++++	++++
E361Q	+++	−	−
H447Q	+++	+++	++++
H447E	− −	−	+
H447N	+	+	+++
H447D	− −	− −	+
H447K	− −	− −	−
H447A	nd	nd	nd

[a] ++++, specific activity equivalent to wild type; +++, 10−100-fold reduced in activity; ++, 500−1000-fold reduced in activity; +, greater than 5000-fold reduced in activity; − −, more than 100 000-fold reduced in activity; −, more than 10 000-fold reduced in activity; nd, not determined. [b] Measured by H_2O_2 formation with HRP coupling. [c] Measured by cholest-4-en-3-one formation at 240 nm.

Consequently, they could not isomerize the 4,5-alkene of the alcohol.

Next, comparisons of mutant activity using cholest-5-en-3-one as substrate were made by measuring the rate of cholest-4-en-3-one appearance at 240 nm. The wild-type enzyme catalyzes the isomerization of the cholest-5-en-3-one intermediate almost as efficiently as it catalyzes oxidation and isomerization of cholesterol. The H447E and H447D mutants isomerized cholest-5-en-3-one 6000−9000-fold more slowly than wild type. As expected from previous work, E361Q did not isomerize cholest-5-en-3-one. Furthermore, within the detection limit the H447K mutant did not isomerize cholest-5-en-3-one, and was at least 10 000-fold reduced in activity from wild type. The H447Q and H447N mutants formed cholest-4-en-3-one from cholest-5-en-3-one at rates close to the wild-type reaction. The reaction product(s) of the mutant catalyzed reactions was (were) analyzed by reversed-phase C-18 HPLC to confirm the identity of the reaction products. The catalytic capability of all the mutants is summarized in Table 1.

Measurement of Catalytic Activity. The Michaelis−Menten parameters of the active mutants using both cholesterol and cholest-5-en-3-one as substrates are reported in Table 2. All experiments with the mutants were conducted under the same conditions and with the same stock solutions as those with the wild-type oxidase, so that a direct comparison of the results between the enzymes could be made easily.

Below pH 4.5, wild type and all of the mutants irreversibly denature. The values of the wild-type, H447Q, and H447N k_{cat}'s with cholest-5-en-3-one as substrate were independent of pH over the range 4.5−10.6. Isomerization by E361Q could not be rescued by increasing the pH.

To study the pH dependence of the oxidation reaction, the catalytic activity was measured by following the appearance of cholest-4-en-3-one, the product of oxidation and isomerization. This was necessary because horseradish peroxidase was inactivated at pHs above 7.5. For wild type, H447Q, and H447N, this did not present a problem because oxidation was rate-limiting and isomerization was independent of pH. For the E361Q mutant, which does not catalyze isomerization, it was necessary to couple the E361Q oxidation with H447N isomerization (using a 10-fold molar excess) and to subtract out the corresponding oxidation activity of H447N at each pH.

The value of k_{cat} with cholesterol as substrate was independent of pH over the range 4.5−7.0 for the wild-type enzyme. Over the range 7.5−10.6, the k_{cat} decreases 2000-fold, and this loss of activity is reversible. The apparent pK_a of k_{cat} is 8.1 for wild type. In contrast, the H447Q- and E361Q-catalyzed oxidation reactions are pH-independent. Although the oxidation activity of H447N was 4400-fold reduced from wild type, the oxidation activity could be increased 10-fold by raising the concentration of hydroxide; the apparent pK_a for this rescue is 9.3 (data not shown).

Measurement of ^2H Transfer. 4β-[^{2}H]Cholest-5-en-3-one was incubated with recombinant H447N or H447Q chox, and the products were purified by reversed-phase HPLC for analysis. The percent deuterium remaining in the product cholest-4-en-3-one was determined by mass spectrometry. The H447N product had 30% D; the H447Q product had 33% D. ^{1}H NMR and ^{13}C NMR spectral analysis of the cholest-4-en-3-one revealed that the deuterium label in the product was incorporated at the 6β-position of cholest-4-en-3-one as it is in the wild-type catalyzed reaction. No deuterium label remained at carbon-4. Previously, we had shown that in the wild-type catalyzed reaction, 30% of the 4β-deuterium was transferred to the 6β-position (*13*).

Measurement of Substrate Deuterium Isotope Effects with 3α-[^{2}H]Cholesterol. As indicated in Table 3, a comparison of wild-type k_{cat} using 3α-protonated cholesterol with that obtained with the 3α-deuterated substrate yielded a primary substrate deuterium isotope effect of 2.2. Within experimental error, the k_{cat}/K_m isotope effect is the same; i.e., K_m is unchanged. The E361Q and H447Q mutants do not show primary isotope effects on k_{cat}. In the case of E361Q, the isotope effect on k_{cat}/K_m is also 1.1. The deuterium isotope effect on k_{cat}/K_m for the H447Q mutant is 0.7.

Measurement of Substrate Deuterium Isotope Effects with 4β-[^{2}H]Cholest-5-en-3-one. For the wild-type reaction, no primary deuterium isotope effects were observed on k_{cat} or k_{cat}/K_m using 4β-deuterated cholest-5-en-3-one. For the H447N and H447Q mutants, a small primary isotope effect is observed on k_{cat}, but not on k_{cat}/K_m (Table 4).

Measurement of Solvent Isotope Effects. For the wild-type reaction, no solvent isotope effects were observed on k_{cat} for oxidation or isomerization. For H447Q and E361Q, small solvent isotope effects were observed on k_{cat} for oxidation (Table 3). There was no isotope effect on isomerization catalyzed by H447Q. For the H447N mutant, there was a solvent isotope effect of 1.5 on isomerization. The 4β-[^{2}H]-cholest-5-en-3-one primary isotope effect measured in D_2O was 1.5, i.e., the same as in H_2O (Table 4). The solvent isotope effect is the same whether cholest-5-en-3-one or 4β-[^{2}H]cholest-5-en-3-one was used as a substrate.

DISCUSSION

Importance of His[447]. The reactions catalyzed by chox are similar to other known enzymes, e.g., glucose oxidase, alcohol dehydrogenases, and Δ^5-ketosteroid isomerase. However, chox catalyzes two *different* reactions in the same active site, in addition to reoxidizing the cofactor to complete the catalytic cycle. The two reactions involving steroid are very different; one is an oxidation of an alcohol to a ketone, and the other is a 1,3-allylic isomerization. Obviously the isomerization is facilitated by oxidation, because formation

Table 2: Michaelis−Menten Rate Constants for Wild-Type and Active Mutant Cholesterol Oxidases

	cholesterol[a]			cholest-5-en-3-one[b]		
	k_{cat} (s^{-1})	K_m (μM)	$(k_{cat}/K_m)_{mut}/(k_{cat}/K_m)_{wt}$	k_{cat} (s^{-1})	K_m (μM)	$(k_{cat}/K_m)_{mut}/(k_{cat}/K_m)_{wt}$
wild type	44 ± 2	3.0 ± 0.4		64 ± 3	6.2 ± 0.7	
E361Q	1.4 ± 0.1	5.4 ± 0.6	0.018	na[c]	na	na
H447Q	0.32 ± 0.01	3.0 ± 0.3	0.0036	81 ± 4	7.1 ± 0.8	1.1
H447N	0.010 ± 0.003	nm[d]	nm	2.3 ± 0.1	3.3 ± 0.4	0.07
H447E	na	na	na	$7 \pm 2 \times 10^{-3}$	nm	nm
H447D	na	na	na	$11 \pm 3 \times 10^{-3}$	nm	nm

[a] Measured by H_2O_2 formation with HRP coupling. [b] Measured by cholest-4-en-3-one formation at 240 nm. [c] Not applicable. [d] Not measured.

Table 3: Solvent and Substrate Isotope Effects on Oxidation of Cholesterol Catalyzed by Wild-Type and Mutant Cholesterol Oxidases[a]

	wild type	E361Q	H447Q
$^{D}(V)_{H2O}$	2.2 ± 0.1	1.11 ± 0.04	1.0 ± 0.1
$^{D}(V/K)$	2.2 ± 0.1	1.11 ± 0.04	0.70 ± 0.1
$(V)_{H2O}/(V)_{D2O}$	1.0 ± 0.1	1.2 ± 0.1	1.3 ± 0.1
$^{D}(V)_{D2O}$	1.9 ± 0.2	0.91 ± 0.05	1.0 ± 0.2

[a] Assayed in 50 mM NaP_i, 0.025% Triton X-100, 3% isopropyl alcohol at 37 °C, pH or pD 7.0. Cholesterol or 3α-[^{2}H]cholesterol was the substrate. Product formation was measured by following H_2O_2 formation with HRP coupling.

Table 4: Solvent and Substrate Isotope Effects on Isomerization of Cholest-5-en-3-one Catalyzed by Wild-Type and Mutant Cholesterol Oxidases[a]

	wild type	H447Q	H447N
$^{D}(V)_{H2O}$	0.86 ± 0.04	1.4 ± 0.1	1.7 ± 0.1
$^{D}(V/K)$	0.86 ± 0.04	1.0 ± 0.1	1.0 ± 0.1
$(V)_{H2O}/(V)_{D2O}$	0.9 ± 0.2	1.0 ± 0.1	1.5 ± 0.2
$^{D}(V)_{D2O}$	1.04 ± 0.03	1.12 ± 0.02	1.5 ± 0.1

[a] Assayed in 50 mM NaP_i, 0.025% Triton X-100, 3% isopropyl alcohol at 37 °C, pH or pD 7.0. Cholest-5-en-3-one or 4β-[^{2}H]cholest-5-en-3-one was the substrate. Product formation was measured by cholest-4-en-3-one formation at 240 nm. These data were corrected for isotopic incorporation in the substrate (0.88 mol of D) as determined by ^{1}H NMR spectroscopy.

of a ketone at carbon-3 increases the acidity of the 4β-proton from ~40 to 12 (*22*). The expected requirements of each reaction for general base and electrophilic catalysis, however, are very distinct. Oxidation should be facilitated by a base, to deprotonate the 3-hydroxyl, though the dienolate intermediate of isomerization should be stabilized by an electrophilic group. A His/Glu/His triad in glucose oxidase positions the glucose and deprotonates the hydroxyl (*7*, *23*). Hydroxysteroid dehydrogenases (both the aldo−keto reductase and the short-chain dehydrogenase/reductase superfamilies) have a Tyr/His pair that serves to position and deprotonate the substrate hydroxyl (*24*). Ketosteroid isomerase isomerizes Δ^5-oxo-steroids to Δ^4-oxo-steroids and employs a tyrosine and an aspartic acid to stabilize formation of the dienolic intermediate (*25*). The pK_a of the phenolic hydrogen is matched to the pK_a of the dienolate oxygen. In the reaction catalyzed by chox, His^{447} is a candidate for general base and electrophilic catalysis. Consideration of the sequential requirement for general base and electrophilic catalysts suggests that histidine has evolved into this position to fulfill the dual roles required for the dual reactions catalyzed. Proton transfer to a neutral imidazole upon oxidation would form imidazolium, a good electrophile for dienolate formation. However, the kinetic competence of the intermediate, cholest-5-en-3-one, to undergo isomerization without prior formation of imidazolium via oxidation brought this interpretation into question and prompted us to investigate the role of His^{447} in chox catalysis.

In the wild-type catalyzed reaction, 3α-hydrogen−carbon bond breaking is at least partially rate-limiting.[3] A primary isotope effect of 2.2 is observed on both k_{cat} and k_{cat}/K_m. Binding of substrate, cholesterol, to the enzyme does not contribute to the rate-determining step, because the k_{cat}/K_m isotope effect is equal to that for k_{cat}. The large value of k_{cat} for isomerization suggests that we are observing the intrinsic isotope effect on oxidation. That is, the steps after 3α-hydrogen transfer (isomerization) are faster than the overall rate of reaction (oxidation plus isomerization). The second-order rate constant, k_{cat}/K_m, for oxidation is 1.4×10^7 M^{-1} s^{-1} and very close to the diffusion-limited rate. Therefore, the rate of 3α-hydrogen abstraction is only marginally slower than substrate binding.

Every amino acid replacement of His^{447} we studied resulted in significant reductions in oxidation activity, thus implicating His^{447} in the catalytic mechanism. Only two mutants, H447Q and H447N, had any catalytic activity, and the activity of H447N was sufficiently low (4400-fold reduced) that we did not measure its oxidation properties in great detail. Perhaps most surprising was the inactivity of H447E and H447D. We expected that these basic residues could act as general bases for oxidation, if present in their ionized forms, and as electrophiles for isomerization, if present in their protonated forms. The inability of either mutant to oxidize and their low isomerization activities suggest that they are present in their protonated forms. Their elevated pK_a's and low isomerization activity hint that His^{447} does not function as a general base or electrophilic catalyst in isolation. The protein environment around mutants Glu^{447}, Asp^{447}, and, by extrapolation, wild-type His^{447} perturbs the pK_a. These mutants and the H447K mutant, constructed to analyze the isomerization reaction, are discussed below. Our inability to express H447A is most likely a result of the instability of the mutant protein, perhaps because the mutation disrupts the hydrogen bond network in the active site.

Active-Site Water Structure of H447Q and H447N Chox. The Gln and Asn substitutions were chosen because their

[3] The oxidation reaction catalyzed by chox utilizes an FAD cofactor, and thus may proceed as a hydride transfer, or it may proceed as two 1 e^- transfer steps, one of which is a hydrogen atom transfer. Both mechanisms would proceed more efficiently with general base catalysis, and from a structural viewpoint, both are feasible. For the sake of simplicity, we will discuss our experiments in reference to the hydride mechanism, although the arguments presented apply equally well to a two-step mechanism, i.e., hydrogen atom transfer followed by fast e^- transfer.

Scheme 2

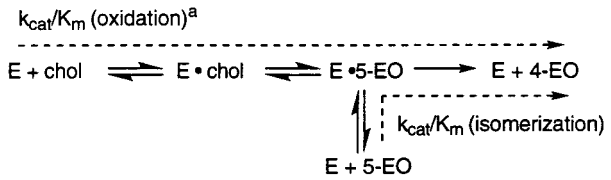

[a] Except for E361Q which releases 5-EO.

side-chain amides are isosteric for Nϵ and Nδ of His. These mutations result in 120-fold and 4400-fold reductions in k_{cat}, respectively. Our prediction based on the wild-type crystal structure was that Nϵ is the nitrogen required for general base catalysis. The difference in oxidation activity between H447Q and H447N confirmed this prediction; the hydrogen bonds between Nϵ of His[447], Wat[541], and the substrate hydroxyl appear critical for catalysis. Substitution of His[447] with Asn forces Wat[541] to move 1.9 Å toward Asn[447] (Yue, K., Kass, I. J., Sampson, N. S., and Vrielink, A., personal communication). The change in position of Wat[541] in turn causes a movement of the remaining waters in the active-site to maintain the hydrogen bonding structure. The shift in position of Wat[541] and the other active site waters suggests that the substrate position will be shifted as well, and that part of the rate decrease is due to a mispositioning of substrate with respect to the FAD.

Although the activity of H447Q is reduced with respect to wild type, we were surprised that substitution of a base with a nonbasic residue did not cause a larger decrease in the catalytic rate. The water structure in the active site of the H447Q mutant is not perturbed relative to wild type, suggesting that the substrate is still positioned correctly (Yue, K., Kass, I. J., Sampson, N. S., and Vrielink, A., personal communication). The simplest explanation for the 120-fold drop in catalytic activity upon Gln substitution is that complete deprotonation of the hydroxyl is not required. That is, the imidazole of His[447] only serves to help delocalize the developing positive charge and is never fully protonated. Although not as efficient as His, Gln[447] could still delocalize the charge that is built up in the transition state through hydrogen bonding. This mechanism is appealing, because a protonated ketone undergoes isomerization much more readily, and presumably the less proton movement there is, the more efficient catalysis will be. However, in the H447Q reaction, there is no primary deuterium kinetic isotope effect observed in the reaction; hydride transfer is no longer rate-limiting (Table 3). Furthermore, the pH profile of the mutant reaction is different than that of wild type. Both of these experiments tell us that the rate-determining step of the H447Q-catalyzed reaction is different than in the wild-type reaction. When the imidazole base is replaced with an amide, the k_{cat} is reduced 120-fold, and transfer of the 3α-hydrogen is no longer rate-limiting.

Comparison of Oxidation and Isomerization Activities. Comparison of the rates for turnover of cholesterol and for turnover of cholest-5-en-3-one in the H447Q-catalyzed reaction allows elimination of possible rate-determining steps (Scheme 2). The k_{cat}/K_m for H447Q-catalyzed isomerization is equal to that of wild type (Table 2), and is 200 times faster than H447Q-catalyzed oxidation. HPLC analysis of the reaction shows that the intermediate cholest-5-en-3-one is not released from the enzyme, but is converted rapidly to cholest-4-en-3-one. Therefore, neither deprotonation of cholest-5-en-3-one, protonation of the dienolic intermediate, nor cholest-4-en-3-one release is rate-limiting in the H447Q reaction. The fact that isomerization is so much faster than oxidation suggests that the k_{cat} for oxidation includes steps prior to isomerization. Hence, the lack of a deuterium primary isotope effect on the k_{cat} for oxidation and the fast rate of isomerization indicate that a step prior to hydrogen transfer, or after hydrogen transfer and before isomerization, becomes rate limiting in the mutant reaction, i.e., a rate-limiting deprotonation of the 3-hydroxyl or the 3-ketone. The solvent isotope effect observed for H447Q-catalyzed oxidation, although quite small, supports this proposal. The lack of a primary deuterium isotope effect on the k_{cat} for oxidation in D_2O clearly shows that 3α-hydrogen−carbon bond breaking and the solvent-sensitive step (presumably, deprotonation of the oxygen) are not in the same kinetic step.

Oxidation in the Mutant Chox Reactions. If deprotonation of the oxygen becomes rate limiting in the H447Q oxidation reaction, what catalytic residue is acting as the base? Examination of the hydrogen-bonding network in the crystal structure (Figure 1) suggests that two species might be contributing to the residual activity of H447Q and thus to catalysis of oxidation. Wat[541] is hydrogen-bonded to Asn[485]. This residue is in turn hydrogen-bonded to Glu[361]. Glu[361] could be acting as the catalytic base for oxidation. Furthermore, the amide side chain of Asn[485] is positioned directly over the N-terminal end of helix 14, and negative charge buildup on Asn[485] could be stabilized by the helix dipole. To investigate the first possibility, we further characterized the kinetic profile of E361Q, a mutant previously prepared to study isomerization. This mutation results in a 30-fold reduction in k_{cat}, transfer of the 3α-hydrogen is not rate-limiting, and the k_{cat} is independent of pH. Thus, the rate-limiting step for E361Q is different than for wild type. The E361Q mutant does not isomerize cholest-5-en-3-one; instead it is released from the enzyme (*13*). Consequently, either cholest-5-en-3-one release, which is not a major pathway for the wild-type reaction, or an oxygen deprotonation step before or after hydrogen transfer becomes rate-limiting. The small solvent isotope effect supports either possibility.

2α,3α-Cyclopropano-5α-cholestan-3β-ol is an irreversible inhibitor of cholesterol oxidase that is active site directed (McCann, A. E., and Sampson, N. S., personal communication). Because the steroid is a tertiary alcohol, it cannot undergo oxidation to the ketone. The mechanism of inactivation appears to be base-catalyzed anionic ring-opening to form a covalent adduct with the FAD. Interestingly, the H447N mutant is not inactivated by the cyclopropyl sterol, H447Q is inactivated 10 times more slowly, and E361Q is inactivated at the same rate as wild type. The inactivation profile of this inhibitor strongly argues that His[447] is required for formation of the anion and that it deprotonates the 3-hydroxyl. Considered together with the kinetic data presented above, it appears that the rate-determining step in the H447Q-catalyzed oxidation of cholesterol is deprotonation of the 3-hydroxyl. This conclusion is further supported by the pH dependence of the H447N reaction. As hydroxide concentration increases, the reaction rate increases. We do not see a similar rescue of the H447Q oxidation activity, perhaps because the water structure of the active site has not been altered by the mutation and there is no room for

hydroxide ion.

It seems reasonable that in the wild-type reaction, both His[447] and Glu[361] catalyze deprotonation of the substrate hydroxyl via Wat[541], perhaps by stabilizing the developing positive charge on Wat[541]. This pair is catalytically efficient, and hydride transfer is rate limiting. Upon mutation of either residue, the remaining residue is left to serve alone and is less catalytically efficient, and the deprotonation of the hydroxyl becomes rate-limiting.

Isomerization in the Mutant Chox Reactions. The wild-type cholesterol oxidase efficiently catalyzes the isomerization of cholest-5-en-3-one to cholest-4-en-3-one. This is quite remarkable considering that if a network between His[447], Glu[361], and Wat[541] acts as the general base for oxidation, and its conjugate acid is the electrophile for isomerization, that when the isomerization reaction is catalyzed without oxidation, i.e., using cholest-5-en-3-one as a substrate, the network is in the 'wrong' protonation state to act as an electrophile. Perhaps the free enzyme can rapidly interconvert between the protonated and neutral forms. Alternatively, it is possible that when cholest-5-en-3-one is generated on the enyzme (by oxidation of cholesterol) the isomerization reaction is faster than if the enzyme binds cholest-5-en-3-one from solution. The k_{cat}/K_m for the latter process is 1×10^7 M^{-1} s^{-1}, approaching the diffusion limit for molecules of their size. The lack of kinetic isotope effects on the wild-type isomerization reaction confirms that chemistry is not rate-limiting for the isomerization reaction. These two considerations suggest that substrate binding and/or product release are rate-limiting in the wild-type catalyzed isomerization of cholest-5-en-3-one. Thus, it is not possible to compare the two rates of isomerization using steady-state kinetics.

The second-order rate constant k_{cat}/K_m for the H447Q-catalyzed isomerization is unchanged from wild type, and there is no primary kinetic isotope effect on k_{cat}/K_m. The activity of this mutant suggests, again, that the electrophilic properties of protonated His[447] are not essential for isomerization. This is in direct contrast to the 1,3-diaxial isomerization catalyzed by ketosteroid isomerase that also utilizes a carboxylate base, and for which evidence of a strong hydrogen bond between the electrophile, Tyr[155], and the dienolate has been obtained (*25*−*27*). In that case, it has been argued that tyrosine is the electrophile because its pK_a is matched to the dienol. In the case of chox, hydrogen bonding by an amide is sufficient to stabilize the formation of the dienolic intermediate, and pK_a matching of the electrophile and the dienol does not appear to be required for efficient catalysis of this reaction at a rate that approaches the diffusion limit.

We can compare the nature of transition states that are not rate-limiting in either the wild-type or the mutant reactions using isotope transfer experiments. We expected that one consequence of mutating the electrophile, i.e., His to Gln, would be that the rate of dienolic intermediate protonation would increase, because the intermediate was poorly stabilized (Scheme 3). This increase in rate could lead to a reduced loss of label in a deuterium transfer experiment compared to wild type, assuming that the rate of exchange of the conjugate acid of Glu[361] is not changed by the mutation. That is, the percentage deuterium transfer from the 4β-position reflects the partitioning between deuteration

Scheme 3

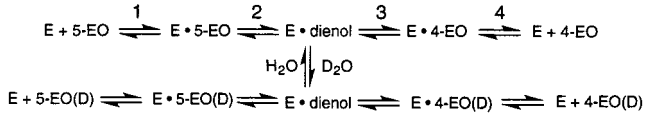

of the dienolic intermediate at C-6 and exchange of the acidic form of the active-site base Glu[361] with solvent protons. The unchanged percentages of deuterium transfer for the H447Q and H447N mutants suggest that these mutations do not affect the ground state of the dienolic intermediate or the transition state for protonation of the dienolic intermediate (Scheme 3, step 3). An alternative interpretation that seems much less likely is that the mutations equally perturb the transition states for exchange and protonation. In the reaction catalyzed by triosephosphate isomerase, mutation of the His electrophile to Gln caused a change in mechanism (*28*). The active-site base Glu[165] acted as both electrophile and base. The fact that we do not see 100% loss of deuterium in the H447Q transfer reaction eliminates this type of mechanism change as a possibility in the chox reaction.

Furthermore, when 4β-[^{2}H]cholest-5-en-3-one was incubated with H447N and H447Q, there was no deuterium remaining at the 4-position of the cholest-4-en-3-one product. Hence, the H447N and H447Q enzymes still stereospecifically remove the 4β-hydrogen from cholest-5-en-3-one. The binding orientation of the steroid is not altered by mutation. This highlights another difference between ketosteroid isomerase and chox. In the wild-type ketosteroid isomerase reaction, the isomerization is not completely stereospecific. This is attributed to alternate binding modes of the substrate (*29*).

The H447Q mutant shows a very small primary isotope effect on k_{cat} upon substitution of deuterium at the 4β-position of cholest-5-en-3-one. We observe 70% washout of the 4β-deuterium label during isomerization in the H447Q reaction. Consequently, deuterium substitution may affect more than a single kinetic step. The absence of isotope effect on k_{cat}/K_m indicates that substrate binding is still rate-limiting. The absence of solvent isotope effect suggests that protonation of the intermediate (step 3) is not rate-limiting, and that any k_{cat} isotope effect is on deprotonation. The small magnitude of the k_{cat} isotope effect and the large errors in measurement preclude further conclusions about the rate-limiting step in the H447Q-catalyzed isomerization. However, the lack of solvent and k_{cat}/K_m isotope effects is consistent with the deuterium transfer experiments described above.

Mutation of His[447] to Asn reduces k_{cat} 30-fold, and both a solvent deuterium isotope effect and a primary isotope effect on k_{cat} with 4β-[^{2}H]cholest-5-en-3-one are observed. The primary deuterium isotope effect on k_{cat} is the same in H_2O and D_2O, 1.5−1.7; the solvent isotope effect is the same with protonated and deuterated substrates, 1.5 and 1.4. In other words, reaction of the deuterated stubstrate in D_2O is 2.4-fold slower than reaction of the protonated substrate in H_2O. This clearly shows that the solvent isotope effect and the primary deuterium isotope effect are on the same kinetic step. Considered together with the deuterium washout partition ratios described above, it appears that deprotonation of the cholest-5-en-3-one (step 2) becomes rate-determining when enzyme is saturated with cholest-5-en-3-one.

It is remarkable that H447N can catalyze isomerization as efficiently as it does with a k_{cat}/K_m of 7×10^5 M^{-1} s^{-1}, considering the disturbance of the water hydrogen-bonding network that has occurred and the serious consequences for oxidation observed. The relatively efficient isomerization catalyzed by H447N and the wild-type rate of H447Q indicate that general acid catalysis is not essential for isomerization of cholest-5-en-3-one. The wild-type rate of H447Q suggests that the rate decrease of H447N is a result of poor positioning of the substrate relative to Glu^{361}. Thus, mispositioning results in a 2 kcal/mol decrease in catalysis. Hydrogen bonding of the cholest-5-en-3-one carbonyl to Nϵ of His^{447} or the side-chain amide of Gln^{447} via Wat^{541} provides sufficient stabilization of the dienolic intermediate for isomerization to proceed efficiently. In the H447N-catalyzed reaction, a 5 kcal/mol increase in the activation barrier to oxidation is observed. If one attributes 2 kcal/mol of this increase to mispositioning of the catalytic residue, the remaining increase in energy, 3 kcal/mol, is equal to the increase observed with the H447Q-catalyzed oxidation reaction. This comparison argues that the energies of the two effects, mispositioning and decrease in basicity, are additive.

The high isomerization activity of H447N and H447Q suggested that H447E and H447D should be excellent catalysts for isomerization. Their complete inability to catalyze oxidation implied that Glu^{447} and Asp^{447} are present in their protonated form. The protonated carboxylic acids should be much better electrophilic catalysts for isomerization than Gln and Asn. However, the specific activities of H447E and H447D are 6000−9000-fold lower than wild type, and significantly lower than H447N and H447Q. The low activities of these mutants support the notion that there is communication between residues 447 and 361. In the mutant, communication between Glu^{361} and Glu^{447} would make it very unfavorable to have the basic forms of both residues present simultaneously; consequently, Glu^{447} is protonated. Although Glu^{447} should be a strong electrophile, once proton transfer to the cholest-5-en-3-one carbonyl is initiated, the developing negative charge on Glu^{447} must perturb the pK_a of Glu^{361} and impair its ability to deprotonate carbon-4. The same reasoning applies to H447D, hence, the low activities of both mutants.

The H447K mutant was constructed to see if Lys could substitute as the electrophile for isomerization. Lys was introduced at position 447 to see if a positively charged electrophile could be accommodated in the active site. The inactivity of H447K clearly shows that this nonconservative substitution for His^{447} is not tolerated.

Summary. The results of our mutagenesis studies suggest that a hydrogen-bonding network involving more than a single basic residue is required for efficient oxidation. It appears that His^{447} is the base for oxidation in the reaction catalyzed by chox and it is assisted by Glu^{361} in a hydrogen-bonding network mediated by Wat^{541} and Asn^{485}. The hydrogen bond network positions the substrate relative to the FAD cofactor, and the active site base(s). Imidazole is utilized because a neutral or positively charged residue is required at this position. A pair of anionic residues would not be present in the correct ionization state for hydroxyl deprotonation, and would shift the pK_a of Glu^{361}, the base for isomerization, in the wrong direction. The introduction of acidic residues at position 447 demonstrated that there is cross-talk between this position and Glu^{361}. The presence of this cross-talk and the relatively high activity of the H447Q mutant indicate that Glu^{361} contributes to general base catalysis during oxidation. The His^{447}, Glu^{361}, Asn^{485}, and Wat^{541} hydrogen bond network is conserved among other oxidases that do not catalyze 1,3-allylic isomerizations. This conservation also suggests Glu^{361} plays a part, structurally and catalytically, in oxidation. Observation of this catalytic tetrad in proteins of unknown function may be diagnostic for an ability to oxidize unactivated alcohols.

In addition, our mutagenesis studies demonstrated that a protonated His^{447} is not required for isomerization. The dienolic intermediate is formed with a hydrogen bond donor, in the absence of an acid catalyst, faster than the rate of substrate diffusing to the enzyme. However, imidazolium could increase the rate of the chemical isomerization steps by several orders of magnitude. This increase would be kinetically invisible in the steady-state. Thus, pK_a matching of the hydrogen-bonding moieties of the electrophile and the intermediate is not obligatory.

ACKNOWLEDGMENT

We thank Prof. Vernon Anderson for his assistance with the equations for fitting the isotope effect data. We thank the reviewers for their helpful suggestions.

REFERENCES

1. Purcell, J. P., Greenplate, J. T., Jennings, M. G., Ryerse, J. S., Pershing, J. C., Sims, S. R., Prinsen, M. J., Corbin, D. R., Tran, M., Sammons, R. D., and Stonard, R. J. (1993) *Biochem. Biophys. Res. Commun. 196*, 1406−1413.
2. Greenplate, J. T., Duck, N. B., Pershing, J. C., and Purcell, J. P. (1995) *Entomol. Exp. Appl. 74*, 253−258.
3. Lange, Y. (1992) *J. Lipid Res. 33*, 315−321.
4. Cavener, D. R. (1992) *J. Mol. Biol. 223*, 811−814.
5. Li, J., Vrielink, A., Brick, P., and Blow, D. M. (1993) *Biochemistry 32*, 11507−11515.
6. Vrielink, A., Li, J., Brick, P., and Blow, D. (1994) in *Flavins and Flavoproteins 1993*, pp 175−184, Walter de Gruyter & Co., Berlin.
7. Kiess, M., Hecht, H. J., and Kalisz, H. M. (1998) *Eur. J. Biochem. 252*, 90−99.
8. Vrielink, A., Lloyd, L. F., and Blow, D. M. (1991) *J. Mol. Biol. 219*, 533−554.
9. Ishizaki, T., Hirayama, N., Shinkawa, H., Nimi, O., and Murooka, Y. (1989) *J. Bacteriol. 171*, 596−601.
10. Ohta, T., Fujishiro, K., Yamaguchi, K., Tamura, Y., Aisaka, K., Uwajima, T., and Hasegawa, M. (1991) *Gene 103*, 93−96.
11. Kass, I. J., and Sampson, N. S. (1995) *Biochem. Biophys. Res. Commun. 206*, 688−693.
12. Sampson, N. S., Kass, I. J., and Ghoshroy, K. B. (1998) *Biochemistry 37*, 5770−5778.
13. Sampson, N. S., and Kass, I. J. (1997) *J. Am. Chem. Soc. 119*, 855−862.
14. Blow, D., Vrielink, A., and Brick, P. (1997) *Curr. Sci. 72*, 477−482.
15. Nomura, N., Choi, K.-P., and Murooka, Y. (1995) *J. Ferm. Bioeng. 79*, 410−416.
16. Sambrook, J., Fritsch, E. F., and Maniatis, T. (1989) *Molecular Cloning: A Laboratory Manual*, 2nd ed., Cold Spring Harbor Laboratory Press, Cold Spring Harbor, NY.
17. Ratcliffe, R., and Rodehorst, R. (1970) *J. Org. Chem. 35*, 4000−4002.
18. Fasman, G. D. (1992) *Practical Handbook of Biochemistry and Molecular Biology*, CRC Press, Boca Raton, FL.
19. Dang, H.-S., Davies, A. G., and Schiesser, C. H. (1990) *J. Chem. Soc., Perkin Trans. 1*, 789−794.

20. Smith, A. G., and Brooks, C. J. W. (1977) *Biochem. J. 167*, 121−129.
21. Schowen, K. B., and Schowen, R. L. (1982) *Methods Enzymol. 87*, 551−606.
22. Hawkinson, D. C., Pollack, R. M., and Ambulos, N. P., Jr. (1994) *Biochemistry 33*, 12172−12183.
23. Hecht, H. J., Kalisz, H. M., Hendle, J., Schmid, R. D., and Schomburg, D. (1993) *J. Mol. Biol. 229*, 153−172.
24. Bennett, M. J., Schlegel, B. P., Jez, J. M., Penning, T. M., and Lewis, M. (1996) *Biochemistry 35*, 10702−10711.
25. Cho, H.-S., Choi, G., Choi, K. Y., and Oh, B.-H. (1998) *Biochemistry 37*, 8325−8330.
26. Zhao, Q., Abeygunawardana, C., Talalay, P., and Mildvan, A. S. (1996) *Proc. Natl. Acad. Sci. U.S.A. 93*, 8220−8224.
27. Zhao, Q., Abeygunawardana, C., Gittis, A. G., and Mildvan, A. S. (1997) *Biochemistry 36*, 14616−14626.
28. Nickbarg, E. B., Davenport, R. C., Petsko, G. A., and Knowles, J. R. (1988) *Biochemistry 27*, 5948−5960.
29. Zawrotny, M. E., Hawkinson, D. C., Blotny, G., and Pollack, R. M. (1996) *Biochemistry 35*, 6438−6442.
30. Kraulis, P. J. (1991) *J. Appl. Crystallogr. 24*, 946−950.

BI982115+